Predicting the high pressure phase transformations using density functional approach

Satish C. Gupta, Jyoti M. Daswani, S. K. Sikka and R. Chidambaram

High Pressure Physics Division, Bhabha Atomic Research Centre, Bombay 400 085, India

During the last decade, there has been an intense feedback between high pressure experiments and theoretical techniques based on the density functional formalism for the analysis of phase transformations. This has resulted in increased accuracy in theoretical computations and they have now acquired predictive capabilities. Some successful examples are discussed. The existing problems and their possible solutions are indicated.

PREDICTIONS of pressure-induced phase transformations in materials from *ab initio* methods are rare. This is because it has been difficult to calculate accurately the small Gibbs free energy differences between different phases (a few mRy/atom or smaller). However, recently, electron band structure techniques based on density functional formalism have acquired such capabilities due to improvements in their formalisms as well as increases in the computational speed. Using these methods, it is now possible to correctly compute the equation of state, the most stable crystal structure of materials, phonon frequencies and other ground state properties[1,2]. The recent calculations on the element thorium, done at Trombay, describe the state of the art. High pressure experiments, done by Vohra and Akella[3], have shown that Th undergoes a fcc to bct phase change at 80 GPa and $V/V_0 = 0.6$. Figure 1 displays the variation of the computed total energy with axial ratio in the bct structure at various compressions[4]. It correctly shows the stability of the fcc ($c/a = 1.414$ in the bct axis) phase up to volume fraction of 0.6, at which the bct structure becomes more stable. The pressure of transition from the fcc to bct phase at 80 GPa agrees very well with the experimental value. In addition, the calculations accurately reproduce the experimental variation of the axial ratio (c/a) with compression in the bct phase (Figure 2) and the equation of state (Figure 3). Also they clearly bring out the important role played by the occupation of the 5f band in this structural transition in thorium.

The experimental techniques, also, have been dramatically improved during the same period. In static high pressure investigations, advances in the diamond anvil cell (DAC) technology coupled with the energy dispersive X-ray diffraction technique (EDXRD) at synchrotron radiation sources have facilitated detection of new phase transformations in solids under megabar pressures[5,6] and this has opened up new vistas for testing theoretical electronic structure calculations[7,8]. In dynamic pressure studies also, a new technique has been developed to detect phase transformations that are accompanied by small volume changes[9]. In this, a phase transformation is inferred from the observation of a discontinuity in the measured sound velocity as a function of peak pressure in the shocked state. The detection, however, like that in other shock wave techniques, is macroscopic in nature and the transition needs to be characterized either by comparison with the

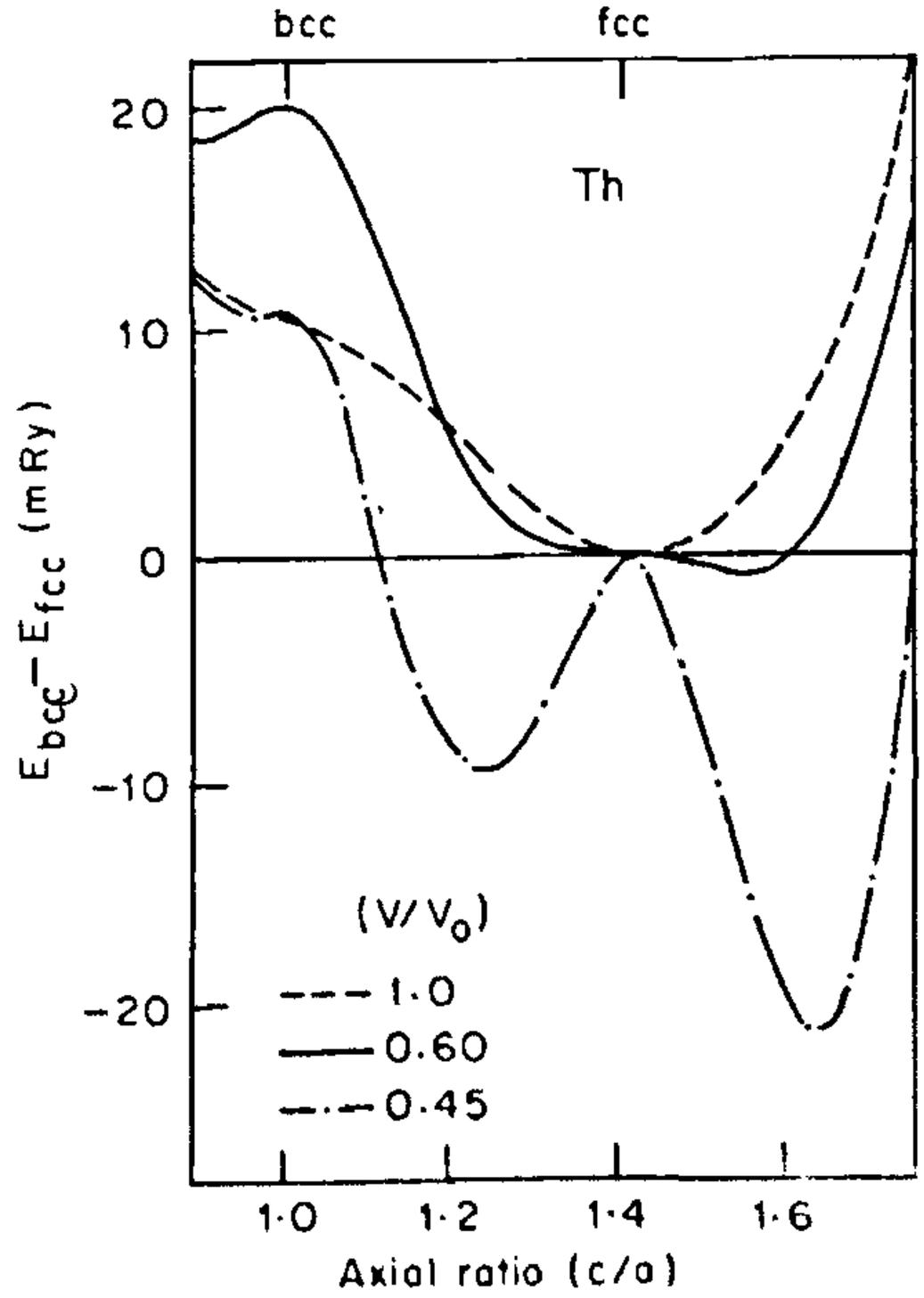

Figure 1. Total energy E_{bct} of thorium in the bct structure (relative to that in fcc phase), calculated as a function of axial ratio c/a. The curves at various compressions are as indicated in the legend (ref 4)

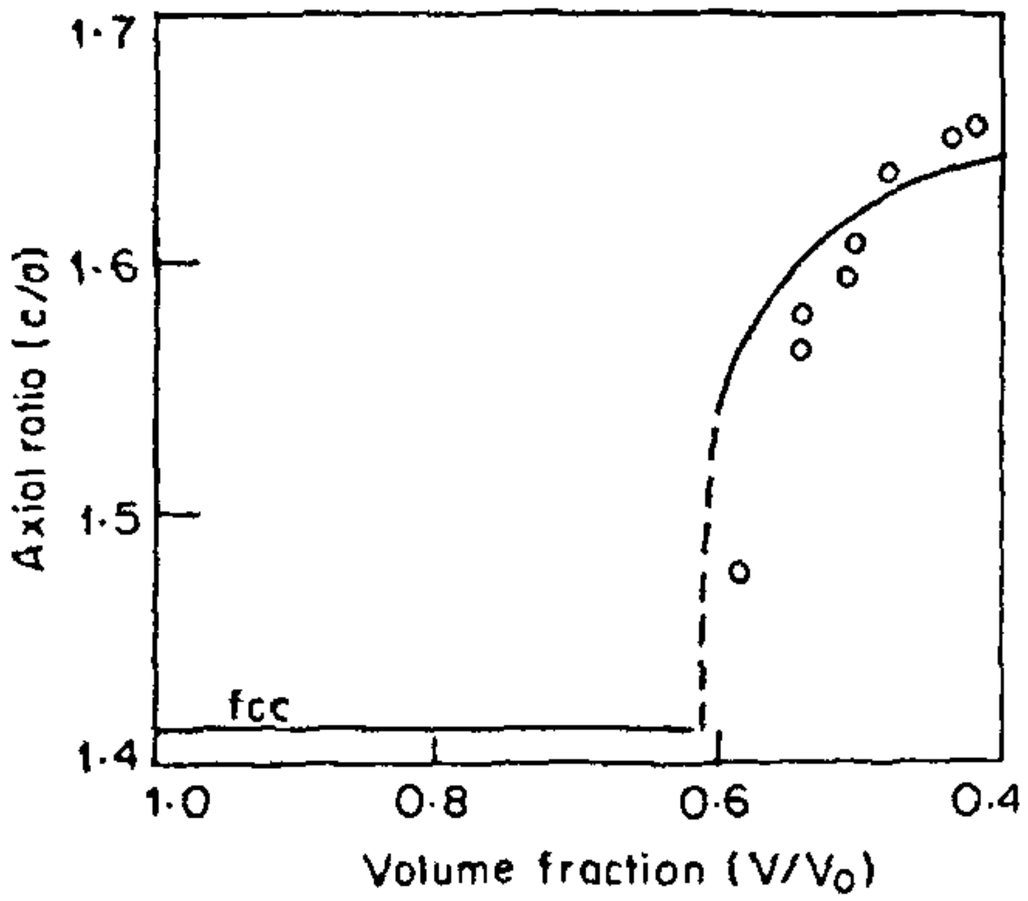

Figure 2. Axial ratio c/a versus V/V_0. The c/a values correspond to the minimum of the total energy curves (see figure 1) at various volume fractions. (ref. 4)

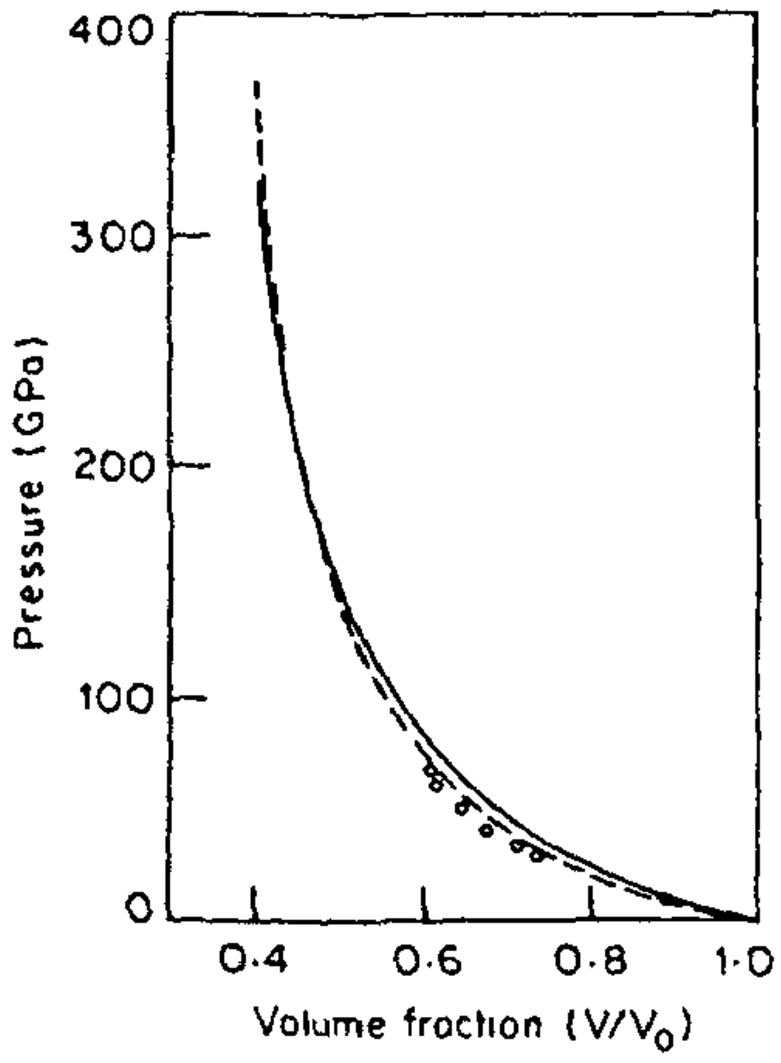

Figure 3. Zero Kelvin isotherm of thorium compared to the experimental data: ——— calculations; – – – and o experiments. (ref. 4)

measurements under static pressure or analysed by band structure calculations[10]. In the absence of measurements under static pressures or in the case of discrepancy between the measurements under static and dynamic pressures, the analysis is heavily based on the band structure calculations[10–15].

In this article, we briefly present the theoretical formalism used for determining the structural stability of crystalline materials under high pressures, and discuss two examples where predictions of pressure-induced phase transformations have been made theoretically and later verified experimentally. One is for elements Si and Mg (ref. 11), and the other is of group IV elements, Ti, Zr and Hf (ref. 12).

Theoretical approach

Under compression, a solid, initially stable in a particular structure at 0 K (we restrict here to 0 K, although the formalism described below can be carried out for any temperature up to $T<0.2\,T_f$), may become more stable in another structure if the enthalpy difference $(\delta E_{12}+P\delta V_{12})$ changes sign at some pressure P_t. Here, δE_{12} is the difference in internal energies of the two structures, which includes the difference between their zero point energies, and δV_{12} is the difference between the volumes of the two structure at pressure P_t. The transition pressure P_t is given by the magnitude of the slope of the common tangent to the internal energy versus volume curves for the two structures. The differences between the zero point energies of various structures, being very small (about 0·1 mRy), are normally negligible. Also, as the change in volume at transition among close-packed structures is usually small (about 1%), the $P\delta V$ term in the Gibbs free energy difference is very small and is again neglected[16]. Therefore, at a given volume, the structure with the lowest internal energy is regarded as the most stable structure.

The calculations for this energy, henceforth referred to as the total energy, are done within the framework of density functional formalism, in which the total energy of a solid with frozen nuclei can be written as (see ref. 17 for details)

$$E=E_{KE}+U+V_{ext},$$

where E_{KE} is the kinetic energy of the interacting electrons, U the electron–electron coulomb repulsion, and V_{ext} the external potential which includes the electrostatic interaction with the fixed nuclei. All these quantities are functionals of the electron density $n(\boldsymbol{r})$.

Minimization of the total energy by the variation of the electron density leads to an effective one electron Schrödinger equation of the form

$$[-\nabla^2+V_{eff}(\boldsymbol{r})]\psi_k(\boldsymbol{r})=\varepsilon_k\psi_k(\boldsymbol{r}) \qquad (1)$$

Here the effective one electron potential is given by

$$V_{eff}(\boldsymbol{r})=2\int\frac{\overline{n(\boldsymbol{r}')}}{|\boldsymbol{r}-\boldsymbol{r}'|}\,d^3\boldsymbol{r}'-2\sum_\mu\frac{Z_\mu}{|\boldsymbol{r}-\boldsymbol{R}_\mu|}+V_{xc}(\boldsymbol{r}), \qquad (2)$$

where Z_μ is the atomic number of the atom centred at $\boldsymbol{R}_\mu$, and the electron density $n(\boldsymbol{r})$ is given by

$$n(r)=\sum_{k}^{occ}|\psi_k(r)|^2 . \tag{3}$$

The first term in eq. (2) is the Hartree term, the second one is the potential due to interaction of the electrons with the nuclei, and the final contribution is the exchange correlation potential. The sum in eq. (3) extends over all occupied states. The exchange correlation potential is given by

$$V_{xc}(r)=\frac{\partial E_{xc}}{\partial n(r)}. \tag{4}$$

Here E_{xc} is the exchange correlation energy, which describes the difference between the true kinetic energy and that of the non-interacting electrons plus the difference between the true interaction energy and that represented by the Hartree term. The general form of this term is not known and it is customary to use local density approximation (LDA)

$$E_{xc}=\int n(r)\,\varepsilon_{xc}(n)\,d^3r \tag{5}$$

where ε_{xc} is the contribution per electron to the total energy of an interacting but homogeneous electron gas of density $n(r)$. Various forms of this are listed in the literature.

Eqs. (1)–(5) are solved self-consistently for the eigenvalues ε_ks and electron density $n(r)$ (so called, a band structure calculation), then the total energy of the system is evaluated from

$$E=\sum_k \varepsilon_k+\sum_\mu Z_\mu \sum_{\mu\neq\nu}\frac{Z_\nu}{|R_\mu-R_\nu|}-$$

$$\int n(r)\,[\varepsilon_{xc}(n(r))-V_{xc}(n(r))]\,d^3r+$$

$$\iint\frac{n(r)\,n(r')}{|r-r'|}d^3r\,d^3r' \tag{6}$$

The pressure, however, may be obtained through

$$P=-\frac{\partial E}{\partial V} \tag{7}$$

or through the use of virial theorem.

Many forms of the band-structure methods, such as *ab initio* pseudopotential method (AP)[18], generalized pseudopotential theory (GPT)[19], linear augmented plane wave method (LAPW)[20], and linear muffin tin orbital method (LMTO) are available[19,21], however AP and LMTO methods are more popular.

Computations are much reduced by employing the frozen core approximation and the force theorem. In the former, the basic idea is to separate E into valence (E_v), core (E_c) and valence–core interaction (E_{v-c}) contributions, i.e.

$$E=E_v+E_c+E_{v-c}.$$

One then assumes that E_c is independent of the structure so that it drops out of the structural energy difference. However, the division into valence and core contribution will alter when some of the core orbitals begin to overlap under compression. In the Andersen force approximation[22], as applied in the LMTO method, one goes a step further by assuming E_{v-c} also to be independent of the structure. The difference in total energy, at a given volume, between two structures (say I and II) is then given by the difference in the sum of one electron eigenvalues, provided the calculation for structure II is done with a frozen potential obtained from a self-consistent calculation for structure I; i.e.

$$\delta E_{I-II}=\delta[\Sigma\varepsilon_k]$$

A muffin tin contribution is also added[2]. This corrects the electrostatic term for the atomic sphere approximation (ASA) in lieu of the actual Wigner Seitz cell and is estimated from the expression

$$E_M\simeq(1.8-\alpha_M)\frac{q_s^2}{S}$$

Here α_M is the Madelung constant and q_s is the charge per atom corresponding to the electron density $n(S)$ at the radius of the atomic sphere, S.

Apart from the atomic numbers, the set of plausible structures is an important input for the structural stability calculations. The probable structures are generally guessed from the use of the principle of corresponding states, which suggests similar phase diagrams for substances containing elements in the same group of periodic table. Symmetry considerations are also useful in deriving the candidate structures. This is based on an analysis of symmetry systematics of pressure-induced phase transitions, suggesting that the transitions are either group–subgroup type, or the intersection group type, where parent and product phases are related through a common subgroup[23,24] (more details are given in ref. 25).

For compounds some clues to the plausible structures for the high pressure phases may be obtained from the quantum structural sorting maps[26] constructed at ambient conditions. These maps essentially consist of two-dimensional displays, where one carefully chosen index (such as ionic radius, Pauling electronegativity, etc.) is plotted against the other for a large database. Figure 4 depicts one such structural sorting map for AB

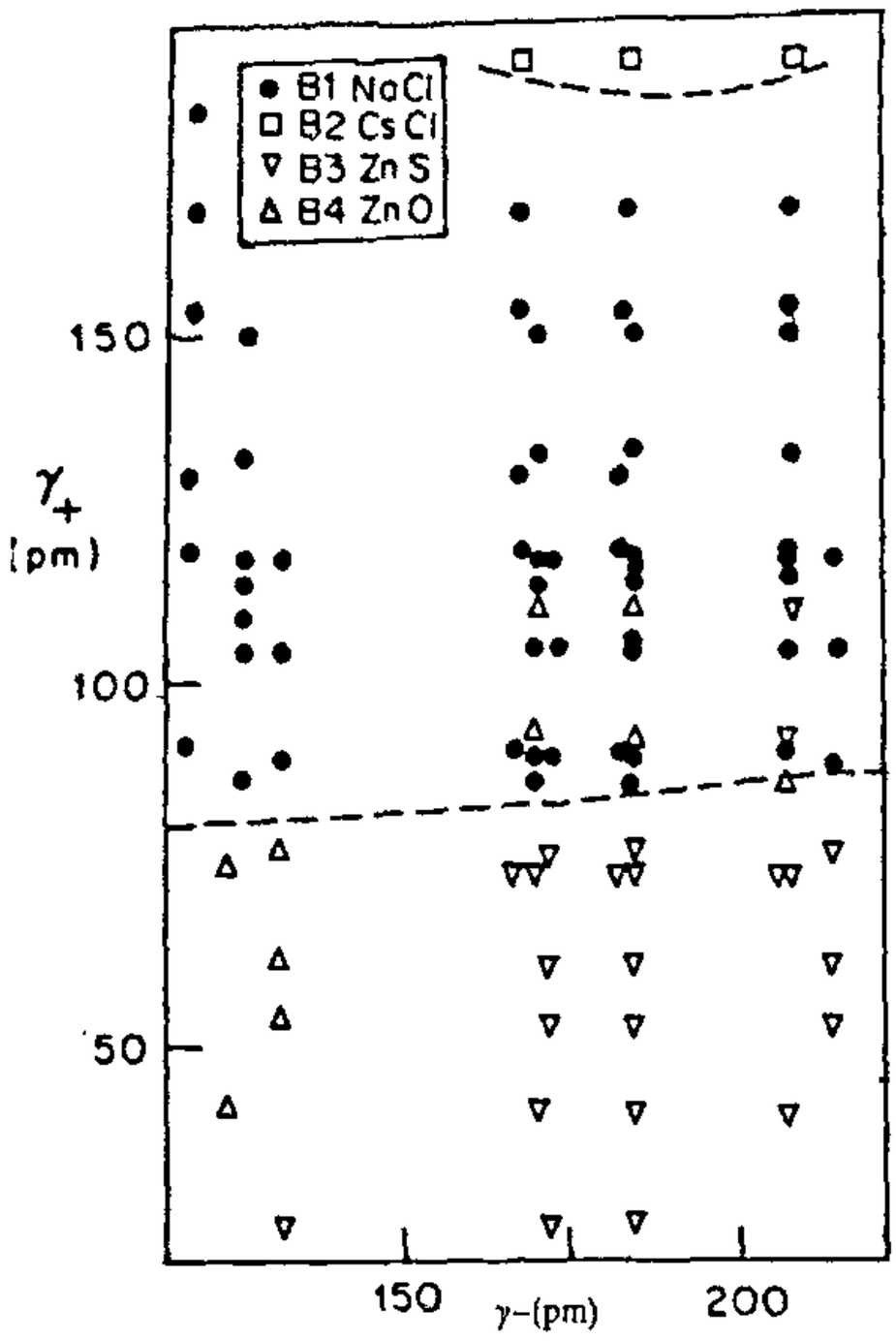

Figure 4. Structural map for AB octet compounds using the crystal radii r_+ and r_-. (ref. 26).

octet compounds based on the crystal ionic radii r_+ and r_-. The map shows clustering of solids with the same crystal structure type. Under pressure the structure after the phase change may be guessed by noting that the new structure will usually have a higher coordination number of the basic building block (e.g. in this case ZnS to NaCl to CsCl sequence under pressure).

Silicon and magnesium

Silicon is a material most studied under pressure, both theoretically and experimentally. Yin and Cohen[1] performed the first successful calculations of a solid-solid transformation on it. Their calculations, using AP band structure method, showed a transformation from the ambient diamond structure to the β-tin structure at 10 GPa; this transition occurs at 12.5 GPa in experiments. McMahan and Moriarty[14] analysed structural phase stability of Si under higher compressions, using both the GPT and LMTO band structure techniques. They predicted three new phase transitions; β-tin to hcp at 41 GPa, hcp to fcc at 76–80 GPa, and fcc to bcc at 250–360 GPa. In addition, they found that the hcp phase would be stable with c/a ratio of 1.67 (larger than the ideal value of 1.633).

Motivated by these predictions, two groups[27] carried out experimental investigations on Si using EDXRD with DAC up to 50 GPa, the highest pressure then achievable. Si showed four structural phase transitions: diamond $\xrightarrow{8\,8\,GPa}$ β-tin $\xrightarrow{16\,GPa}$ primitive hexagonal (ph) $\xrightarrow{36\,GPa}$ Si(VI) $\xrightarrow{40\,GPa}$ hcp. Although Si did transform to the hcp phase of c/a ratio 1.67 around 40 GPa, as predicted earlier, before that it showed two other phase changes. The primitive hexagonal and Si(VI) (later shown to be the X-phase[28]) were found for the first time in an elemental solid. They were not anticipated by theory as these were not included in the analysis. The later calculations, however, rationalized the existence of the ph phase[29,30] (Figure 5) and also found that the transitions, β-tin to ph and ph to hcp were driven by soft phonon modes[23,29]. This picture, also, has been verified recently by neutron scattering measurements on alloys of Sn with In[31]. More recent experiments on Si, performed to much higher pressure[7], found hcp to fcc structural transformation at 79 GPa, again in excellent agreement with the calculations.

McMahan and Moriarty[14] predicted two new phase transitions in Mg: hcp to bcc at 50–57 GPa and bcc to fcc at 180–790 GPa. The first hcp–bcc phase change was found in DAC experiments, at 50 GPa, in excellent agreement with the prediction[32].

Titanium, zirconium and hafnium

Our chief motivation for performing electronic structure calculations on these materials, initially, was to

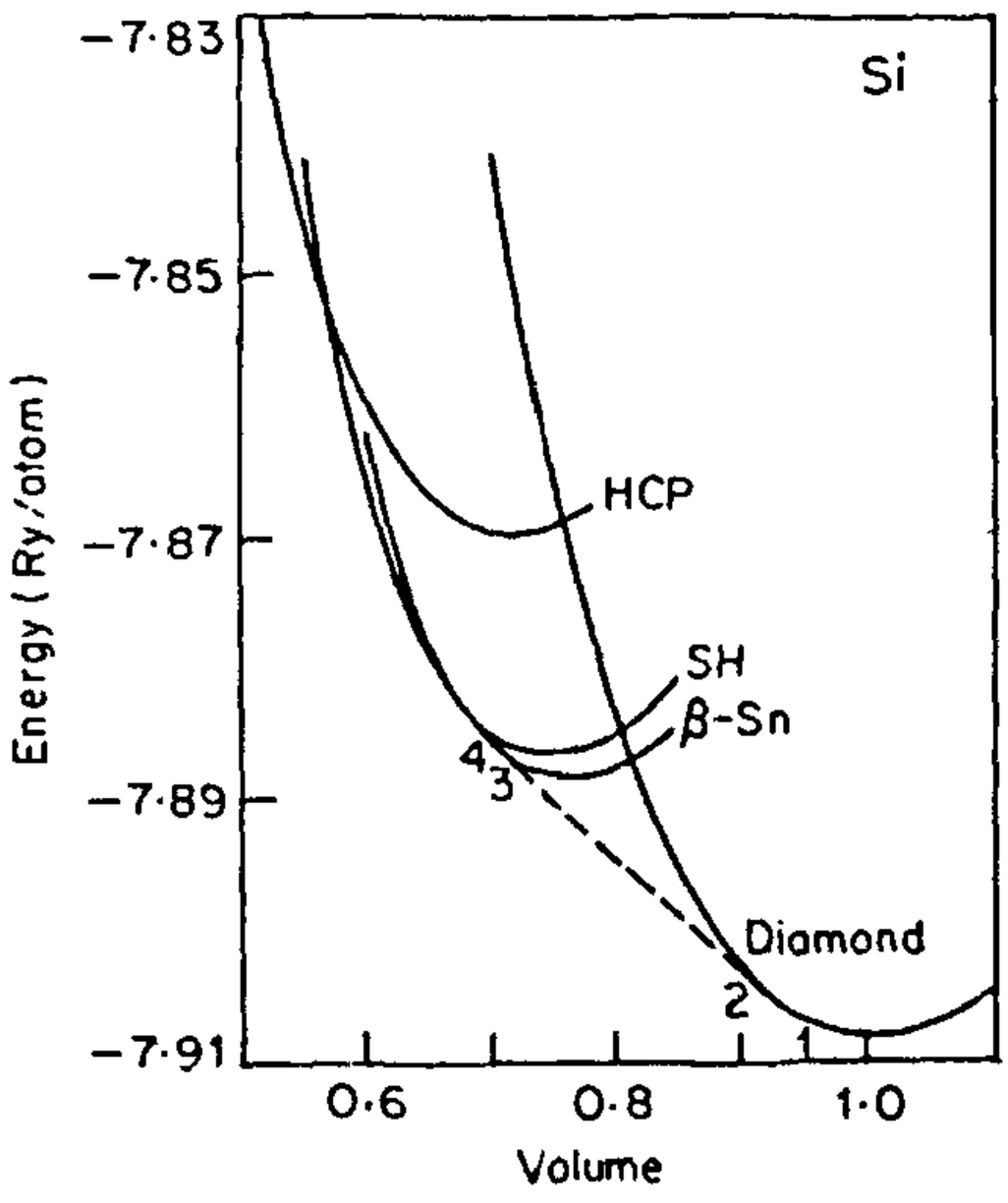

Figure 5. Total energy for various structures of Si versus V/V_0. (ref. 29).

understand the cause of the discontinuities observed in the plots of the experimental shock velocity (U_s) versus particle velocity (U_p) data on them at 17, 26 and 40 GPa respectively[33]. There have been many speculations regarding them. McQueen *et al.* assumed that these were due to an α (hcp) to β (bcc) transition, based on the observation of β phase in the shock recovered samples of Ti. Kutsar and German[34] associated these discontinuities with the α–ω (ω—a three atom simple hexagonal structure) phase change as they found the ω phase in the shock recovered samples of Ti and Zr loaded to the pressures in the vicinity of the above shock discontinuities. Further, Carter[35] speculated that these could be due to some electronic transitions. Our other motivation was to examine the effect of s–d electron transfer, which is expected to result from lowering of the d band with respect to the s band under pressure in these materials. Because of the increased d populations, these materials are expected to assume the bcc structure of the elements next to the right of them in the same period.

The calculations were performed using the semi-relativistic LMTO band structure method. The electronic configurations employed were [Ar] $(3d4s4p)^4$, [Kr] $(4d5s5p)^4$ and [(Xe) $4f^{14}$] $(5d6s6p)^4$ for Ti, Zr and Hf, respectively; their cores (indicated within '[ ]' here) were kept 'frozen'. At a number of volumes, self-consistent calculations were performed for the fcc structure and the energy differences between hcp, bcc and ω structures with reference to the fcc structure were calculated using the Andersen force theorem[22] as described above. The ω structure, which is of AlB_2 simple hexagonal type with two non-equivalent type[36,37] of atoms, was treated as a compound with equal spherical radii for both the kinds of atoms. The c/a ratios for the hcp and ω structures were kept fixed for all compressions, as these do not vary much in experiments. The calculated structural energy differences for the α, β and ω structures with respect to the fcc structure for Zr, Ti, and Hf are shown in Figures 6, 7 and 8, respectively.

In Zr, we correctly found the α structure to be the most stable one at normal volume and under compression the first transition was α–ω at 5 GPa (experimental transition pressure ranges 2–6 GPa[37]). In addition, we found a new ω–β structural transition at 11 GPa. This prediction was subsequently confirmed using EDXRD measurements in DAC done at Cornell[8] and the ω–β transition was found at 30 GPa. The difference between the calculated and experimental transition pressures may be attributed to the assumption of equal spherical radii of the two non-equivalent type of atoms in the ω structure and to the ASA approximation in the LMTO method.

In Ti, our calculations showed the ω structure to be the most stable, at normal volume and suggested no ω–β structural transition under compression up to

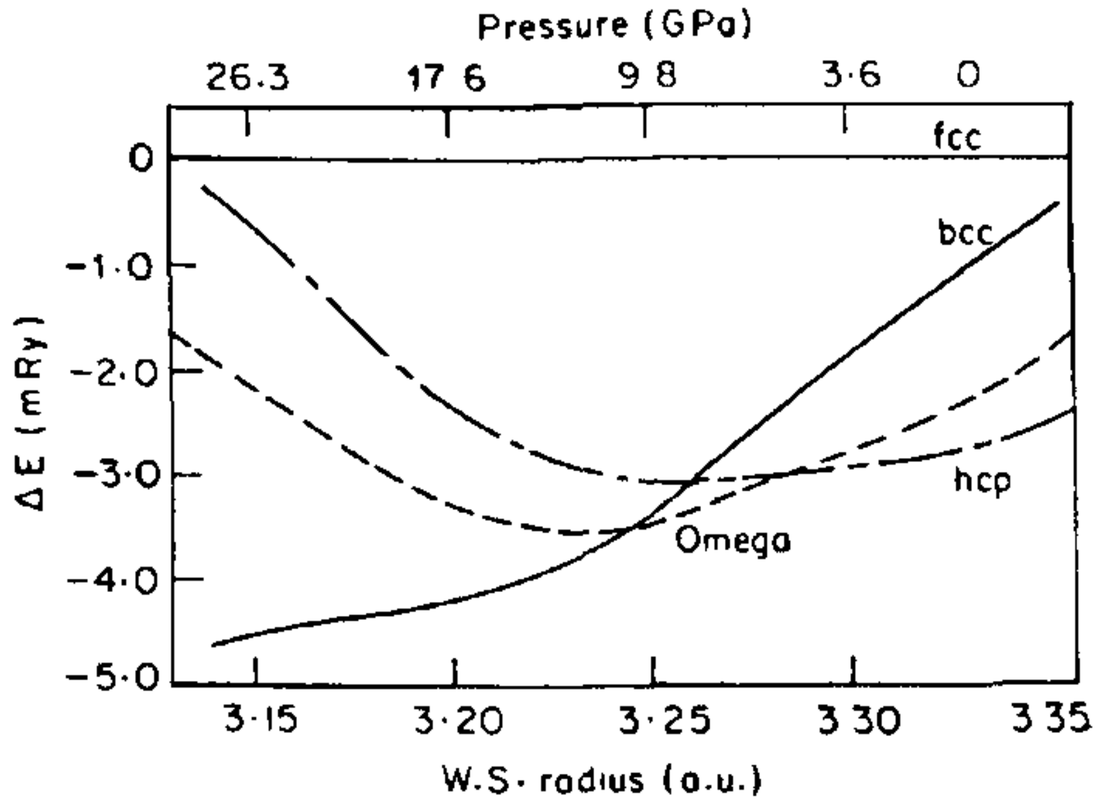

Figure 6. Structural energy differences for Zr. (ref. 15).

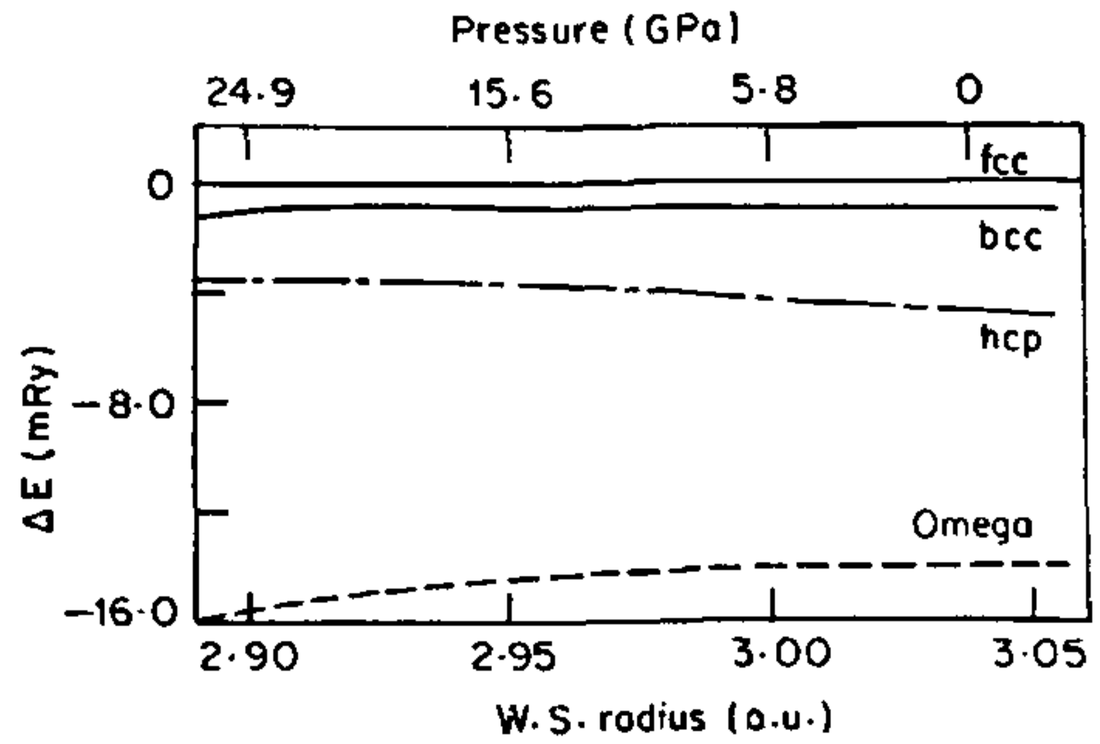

Figure 7. Structural energy differences for Ti. (ref. 38).

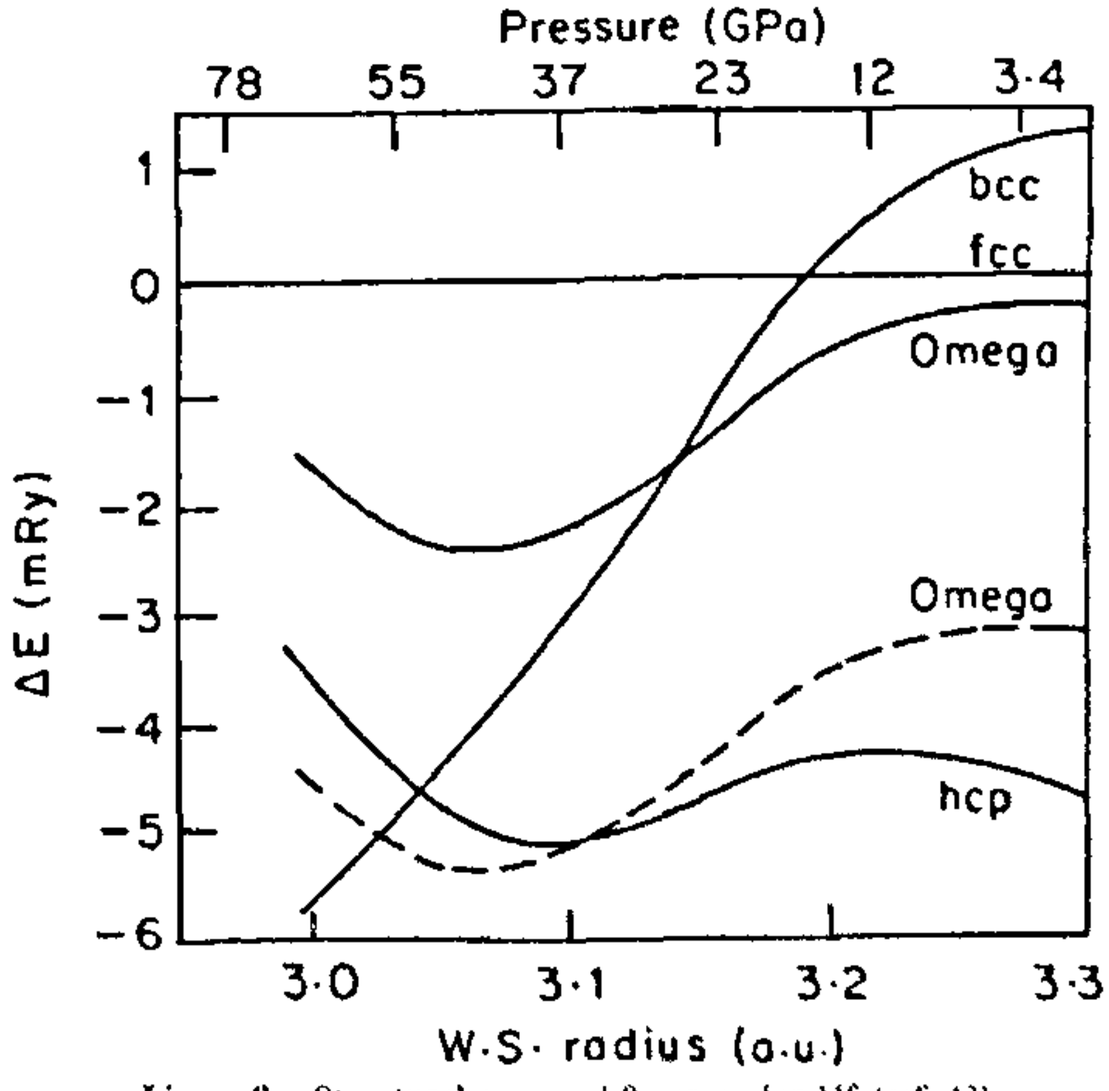

Figure 8. Structural energy differences for Hf (ref. 43).

26 GPa[38]. Although Ti occurs in α phase at normal volume and temperature, the linear extrapolation of the experimental α–ω phase line (which has a negative slope) to low temperatures indicates the ω phase to be stable below 62 K; which is in agreement with our calculations, as these are for 0 K. Again high pressure EDXRD experiments do not find ω–β transition in this material[38,39]. The absence of ω–β transition in our calculations led us to agree with Al'tshuler *et al.*[40] that the initial segment of the U_s–U_p plot of this material is not well established. Shock experiments done subsequently have supported this[41]. The detection of β phase in the shock recovered samples of Ti was ascribed by us to the heterogeneous heating of Ti subjected to high strain rates. The locally heated shear bands could take the material to the high temperature β phase. The presence of shear bands in Ti has also been detected now[42].

Our calculations[43] in Hf showed the stability of α phase at normal volume, and predicted an α–β transition at 51 GPa. However, a α–ω–β structural transition sequence was observed in experiments done simultaneously. This disagreement, as well might be for the same reasons, stated above for Zr. However, by lowering the ω curve by 3 mRy (6% of the Madelung correction, a procedure adopted by others[44] earlier, as this correction is not well established in theory), we found the α–ω transition to occur at 36 GPa and ω–β transition at 55 GPa, which is in line with the experiments. To this extent the LMTO method is deficient for structural stability analysis. The transition pressure for the α–ω phase transition is close to the transition pressure of the shock discontinuity in this material, which suggests that the shock anomaly in this material, near 40 GPa (44.5 GPa according to Al'tshuler), occurs because of this α–ω phase transition.

The transition to β phase in Zr and Hf under high pressures, as expected, also confirmed the correlation between the crystal structure and the d electron population in transition metal series[2,45]. Under compression, the d occupancy increases in these elements and they tend to have the structure of the next elements. The occurrence of the ω and β phases in Hf at higher pressures than in Zr may also be understood as the d electron number in Hf is 2.33 compared to 2.54 in Zr at normal volume. Ti, on the other hand, does not transform to β phase under compression even up to 87 GPa. This is because, the hard core repulsion which sets, is higher for Ti, and this does not favour the bcc structure[46].

Discussion

The above examples, where the successful predictions were made prior to the experiments, illustrate the capabilities of the present day band structure methods based on the density functional formalism. Despite such successes of these methods there are problems: (i) although, the agreement between the predicted and experimental pressure of transition between close packed structures is remarkably good, this agreement for less close packed structures is only fair. Here, use of full potential LMTO method in which ASA approximation is not made, may improve the agreement[47] and (ii) the band structure methods can determine the most stable structure from the chosen candidate structures, but cannot discover the structure that has the lowest free energy. This problem, so far tackled by intelligent search, may be solved in the future by the use of density functional molecular dynamics calculations in which the equilibrium structure emerges naturally out of the computations[48]. This method has so far been used for examining the structural stability of small clusters and its extension to ordered solids is a possibility, especially after the development of massively parallel computing techniques[49,51]. This will also be extremely useful in understanding the mechanism of pressure-induced phase changes[52]; as of now, the path of the transformation has to be guessed.

It may be pointed out that not all the theoretical predictions have been supported by experiments done later on. For example, in case of the triple bonded diatomic nitrogen, it was shown[53] that it should transform to a single bonded form at 50 GPa. However, Raman data[54] indicated the existence of N_2 up to 180 GPa. This discrepancy is attributed not to the failure of the theory but to the metastability of N_2 up to the pressure of the experiment, as under a shock pressure above 30 GPa (temperature–7000 K) N_2 is believed to dissociate[55].

Similarly in Mo, the postulation of bcc to hcp

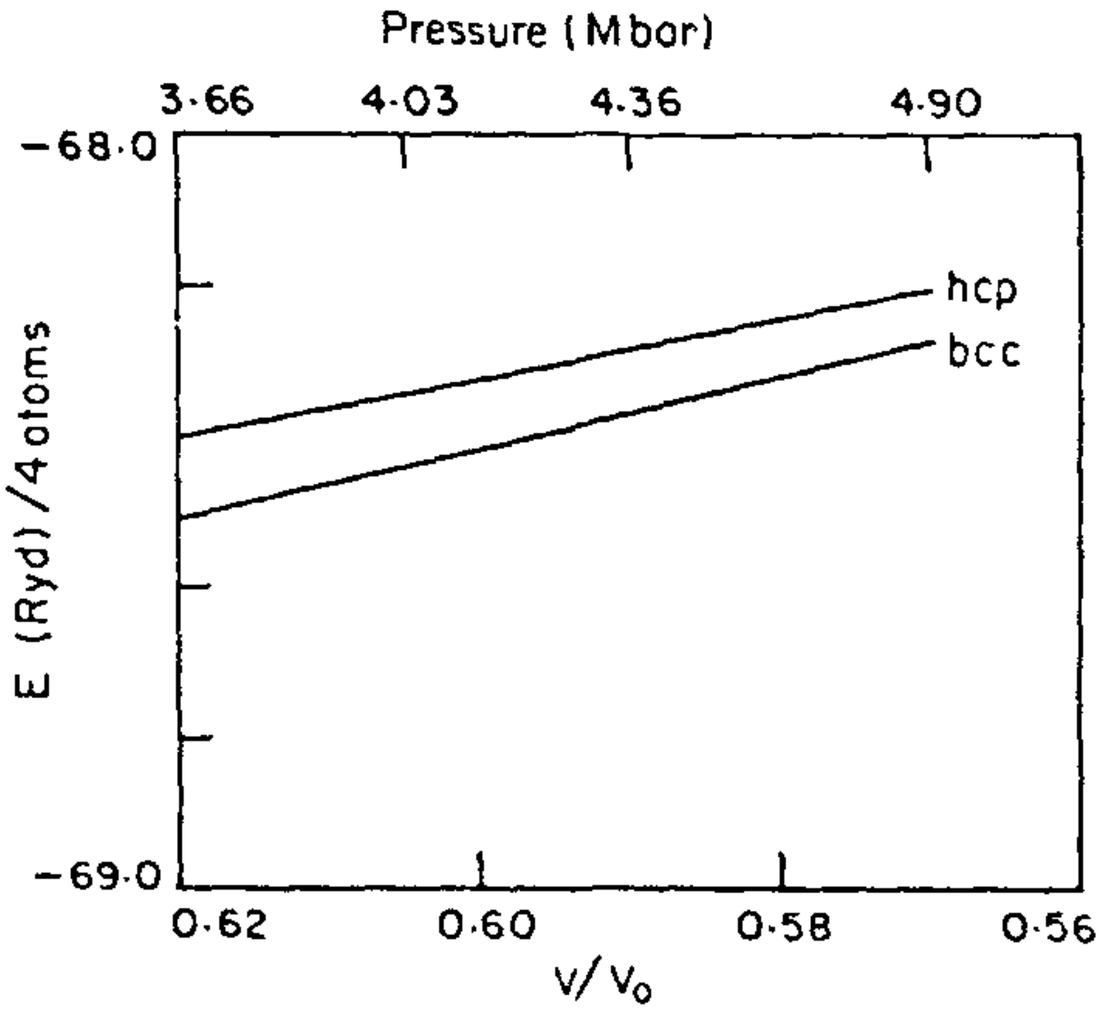

Figure 9. Calculated valence energy for bcc and hcp structures. (ref. 57).

transition at 320 GPa by using the Andersen force theorem[10] has not been found to occur in experiments up to 560 GPa[56]. However, more accurate theoretical calculations done afterwards are in agreement with the experiments[57] (see Figure 9).

The current limit of the accessible pressures with DAC is about 500 GPa. This limit is expected to increase with the further miniaturization of diamond anvil cell. Ruoff and Luo[58] suggest that diamond anvils with 4 μm flats should produce about 1000 GPa pressure. The upper limit of the achievable pressure might be limited, either by plastic flow in anvils or by a phase transition in diamonds, such as, an insulator to metal transition, estimated to occur around 900 GPa under uniaxial stress[58] or by a structural transition to the BC(8) structure, theoretically predicted to be at 1100 GPa[59]. With the increased accessibility of pressure in experiments, coupled with band structure methods, one hopes to witness more intense and exciting interplay between experiments and theory.

1. Yin, M. T. and Cohen, M. L., *Phys. Rev. Lett.*, 1980, **45**, 1004–1007.
2. Gupta, S. C., in *Shock Compression of Condensed Matter—1991* (ed. Schmidt, S. C., Dick, R. D., Forbes, J. W. and Tasker, D. G.), Elsevier, Amsterdam, 1992, pp. 157–163; Skriver, H. L., *Phys. Rev.*, 1985, **B31**, 1909–1923.
3. Vohra, Y. K. and Akella, J., *Phys. Rev. Lett.*, 1991, **67**, 3563–3566.
4. Rao, R. S., Godwal, B. K. and Sikka, S. K., *Phys. Rev.*, 1992, **B46**, 5780–5782.
5. Vohra, Y. K., Brister, K. E., Weir, S. J., Duclos, S. J. and Ruoff, A. L., *Science*, 1986, **231**, 1136–1138.
6. Mao, H. K., Wu, Y., Shu, J. F., Hemley, R. J. and Cox, D. E., *Solid State Commun.*, 1990, **74**, 1027–1029.
7. Duclos, S. J., Vohra, Y. K. and Ruoff, A. L., *Phys. Rev.*, 1990, **B41**, 12021; *Phys. Rev. Lett.*, 1987, **58**, 775–777.
8. Xia, H., Duclos, S. J., Ruoff, A. L. and Vohra, Y. K., *Phys. Rev. Lett.*, 1990, **64**, 204–207.
9. Brown, J. M. and McQueen, R. G., *J. Geophys. Res.*, 1986, **91**, 7485–7494.
10. Hixson, R. S., Boness, D. A., Shaner, J. W. and Moriarty, J. A., *Phys. Rev. Lett.*, 1989, **62**, 637–640.
11. McMahan, A. K., Skriver, H. L. and Johansson, B., *Phys. Rev.*, 1981, **B23**, 5016–5029.
12. Gyanchandani, J. S., Gupta, S. C., Sikka, S. K. and Chidambaram, R., in *Shock Waves in Condensed Matter—1987* (eds. Schmidt, S. C. and Holmes, N. C.), Elsevier, Amsterdam, 1988, pp. 147–150.
13. Gupta, Satish, C., Sikka, S. K., Godwal, B. K. and Chidambaram, R., in *Physics of Materials* (ed Yussouff, M.), World Scientific, Singapore, 1987, pp. 46–50.
14. McMahan, A. K. and Moriarty, J. A., *Phys. Rev.*, 1983, **B27**, 3235–3251.
15. Gyanchandani, J. S., Gupta, S. C., Sikka, S. K. and Chidambaram, R., *High Pressure Res.*, 1990, **4**, 472–474.
16. Moriarty, J. A., *Phys. Rev.*, 1973, **B8**, 1338–1345.
17. Cohen, M. L., *Phys. Scr.* T1, 1982, 5.
18. Godwal, B K., Sikka, S. K. and Chidambaram, R., *Phys. Rep.*, 1983, **102**, 121–197.
19. Moriarty, J A, *Phys. Rev.*, 1982, **B26**, 1754–1779.
20. Andersen, O. K., *Phys. Rev.*, 1975, **B12**, 3060–3083.
21. Skriver, H. L., *LMTO Method*, Springer, Berlin, 1984.
22. Makintosh, A. R. and Andersen, O. K., in *Electron at Fermi Surface* (ed. Springford, M), Cambridge University Press, Cambridge, 1980, pp. 149.
23. Sharma, S. M. and Sikka, S. K., *J. Phys. Chem. Solid*, 1985, **46**, 477–479.
24. Mailhiot, C. and McMahan, A. K., *Phys. Rev.*, 1991, **B44**, 11758–11791.
25. Chidambaram, R. and Gupta, S. C., to be published.
26. Burdett, J. K., Price, G. D. and Price, S. L., *Phys. Rev.*, 1981, **B24**, 2903–2912.
27. Olijnyk, H., Sikka, S. K. and Holzapfel, W. B., *Phys. Lett.*, 1984, **A103**, 137–140; Hu, J. Z. and Spain, I. L., *Solid State Commun.*, 1984, **51**, 263–266.
28. Vijaykumar, V. and Sikka, S. K., *High Pressure Res.*, 1990, **4**, 306–308.
29. Chang, K. J. and Cohen, M. L., *Phys. Rev.*, 1985, **B31**, 7819–7826; *Phys. Rev.*, 1984, **B30**, 5376–5378.
30. Needs, R. and Martin, R., *Phys. Rev.*, 1984, **B30**, 5390–5392.
31. Ivanro, A. S., Rumiantsev, A. Yu., Mitrotanov, N. L. and Alba, M., *Physica*, 1991, **B174**, 79–82.
32. Olijnyk, H. and Holzapfel, W. B., *Phys. Rev.*, 1985, **B31**, 4682–4683.
33. McQeen, R. G., Marsh, S. P., Taylor, J. W., Fritz, J. N. and Carter, W. J., in *High Velocity Impact Phenomena* (ed. Kinslow, R.), Academic, New York, 1971, pp. 293–417.
34. Kutsar, A. R. and German, V. N., Proceedings of the 3rd International Conference on Titanium, Moscow, 1976.
35. Carter, W. J., in *Metallurgical Effects of High Strain Rate* (eds. Rohde, R. W., Butcher, R. M., Holland, J. R. and Carnes C. H.), Plenum, New York, 1973, pp. 171–184.
36. Gyanchandani, J. S., Gupta, S. C., Sikka, S. K. and Chidambaram, R., *J. Phys., Condens. Matter*, 1990, **2**, 301–305.
37. Sikka, S. K., Vohra, Y. K. and Chidambaram, R., *Prog. Mater. Sci.*, 1982, **27**, 245–310.
38. Gyanchandani, J. S., Gupta, S. C., Sikka, S. K. and Chidambaram, R., in *Shock Compression of Condensed Matter—1989* (eds. Schmidt, S. C., Johnson, J. N. and Davidson, L. W.), North-Holland, Amsterdam, 1990, pp. 131–134.
39. Xia, H., Parthasarathy, G., Luo, H., Vohra, Y. K. and Ruoff, A. L., *Phys. Rev.*, 1990, **B42**, 6736–6738.
40. Al'tshuler, L. V., Bakanova A. A., Dudoladov, I. P., Dynin, E. A., Trunin, R. F. and Chekin, B. S., *Zh. Prikl. Mekh, Tekh Fiz.*, 1981, **2**, 3–34.
41. Shaner, J. W., 1989, private communication.
42. Holt, W. H., Mock, W., Soper, W. G., Coffey, C. S., Ramachandran, V. and Armstrong, R. W., in *Shock Compression of Condensed Matter—1989* (eds. Schmidt, S. C., Johnson, J. N. and Davidson, L. W.), North-Holland, Amsterdam, 1990, pp. 915–918.
43. Gyanchandani, J. S., Gupta, S. C., Sikka, S. K. and Chidambaram, R., *J. Phys., Condensed Matter*, 1990, **2**, 6457–6459.
44. McMahan, A. K., *Phys. Rev.*, 1984, **B29**, 5982–5985.
45. McMahan, A. K., *Physica*, 1986, **B139&140**, 31–41.
46. Gyanchandani, J. S., Sikka, S. K. and Chidambaram, R., in *Recent Trends in High Pressure Research*, Proceedings of XIII AIRAPT International Conference on High Pressure Science and Technology (ed. Singh A. K.), Oxford & IBH, New Delhi, 1992, pp. 331–334.
47. Metfessel, M., Rodriguez, C. O. and Andersen, O. K., *Phys. Rev.*, 1989, **B40**, 2009–2012.
48. Car, R. and Parrinello, M., *Phys. Rev. Lett.*, 1985, **55**, 2471–2474.
49. Andreoni, W. and Pastore, W., *Phys. Rev.*, 1990, **B41**, 10243–10246.
50. Andreoni, W, in *Progress in Electron Properties of Solids* (eds. Doni, E., Girlanda, R., Pastori, Parravicini, G. and Quattropani, A, Kluwer Academic, Netherlands, 1989, p. 27.
51. Brommer, K. D., Needels, M, Larson, B. E. and Joannopoulos, J. D., *Phys. Rev. Lett.*, 1992, **68**, 1355.

52. Sankaran, H., Sharma, S. M. and Sikka, S. K., *J. Phys., Condens. Matter*, 1992, **4**, L61–L66.
53. McMahan, A. K. and LeSar, R., *Phys. Rev. Lett.*, 1985, **54**, 1929–1932; Mailhiot, C., Yang, L. H. and McMahan, A. K., (preprint) to be published.
54. Reichlin, R., Schiferl, D., Martin, S., Vanderborgh, C. and Mills, R. L., *Phys. Rev. Lett.*, 1985, **55**, 1464–1467; Bell, P. M., Mao, H. K. and Hemley, R. J., *Physica*, 1986, **B139&140**, 16–20.
55. Radousky, H. B., Nellis, W. J., Ross, M., Hamilton, D. O. and Mitchell, *Phys. Rev. Lett.*, 1986, **57**, 2419–2422.
56. Ruoff, A. L., in *Recent Trends in High Pressure Research*, Proceedings of XIII AIRAPT Int. Conf. on High Pressure Science and Technology (ed. Singh, A. K.), Oxford & IBH, New Delhi, 1992, pp. 769–778.
57. Sikka, S. K., Godwal, B. K. and Rao, R. S., *High Pressure Res.*, 1992, **10**, 707–709.
58. Ruoff, A. L. and Luo, H., in *Recent Trends in High Pressure Research*, Proceedings of XIII AIRAPT Int. Conf. on High Pressure Science and Technology (ed. Singh, A. K.), Oxford & IBH, New Delhi, 1992, pp. 779–781.
59. Biswas, R., Martin, R. M., Needs, R. J. and Nielsen, O. H., *Phys. Rev.*, 1984, **B30**, 3210–3213.

11 December 1992; accepted 18 January 1993